

Nonlocal hydrodynamic phonon transport in two-dimensional materials

Man-Yu Shang and Jing-Tao Lü

*School of Physics and Wuhan National High Magnetic Field Center,
Huazhong University of Science and Technology, Wuhan 430074, P. R. China*

We study hydrodynamic phonon heat transport in two-dimensional (2D) materials. Starting from the Peierls-Boltzmann equation with the Callaway model, we derive a 2D Guyer-Krumhansl-like equation describing non-local hydrodynamic phonon transport, taking into account the quadratic dispersion of flexural phonons. In addition to Poiseuille flow, second sound propagation, the equation predicts heat current vortices and negative nonlocal thermal conductance in 2D materials, which is common in classical fluid but has not yet been considered in phonon transport. Our results also illustrate the universal transport behavior of hydrodynamics, independent of the type of quasi-particles and their microscopic interactions.

I. INTRODUCTION

Macroscopic collective behavior emerges from microscopic many-body interactions between individual degrees of freedom comprising the system. Hydrodynamics is one of such macroscopic phenomena. It could originate from different kinds of microscopic interactions in different materials, ranging from classical gases and liquids, to crystal solids¹⁻¹², and to cold atomic gases¹³ or hot nuclear matter¹⁴. Although the microscopic inter-particle interactions are of different nature, the hydrodynamic behaviors are universal. They can be described by similar hydrodynamic equations. These equations can normally be derived from the microscopic equations of motion by considering physical quantities that are conserved during the inter-particle collisions, i.e., (crystal) momentum, energy or particle number.

Although hydrodynamic flow in classical gases and liquids is a common process that can be observed in everyday life, to observe hydrodynamic transport of (quasi-)particles in crystalline solids is much more difficult. Conservation of crystal momentum is required during the inter-particle collisions. This needs high quality samples to reduce extrinsic scatterings with impurities. It also requires that the intrinsic scattering between quasi-particles to be normal (N-process), which conserves the crystal momentum, instead of Umklapp (U-process), which does not. Furthermore, the hydrodynamic feature is prominent in spatial confined samples like one-dimensional (1D) or two-dimensional (2D) materials¹⁵⁻¹⁷, which raises further challenges in their fabrication and characterization.

Due to these limitations, studies on the hydrodynamic transport of quasi-particles in solid state system are scarce. Recently, experimental and numerical signatures of hydrodynamic electron^{4-6,12,18-25} and phonon^{8,10,11,26-30} transport in 2D materials have been reported. For electron transport, negative nonlocal resistance⁴, violation of Wiedemann-Franz law⁵ and large negative magnetoresistance¹⁸ have been experimentally observed and theoretically explained^{12,19,21-23}.

Considering the universal behaviour of hydrodynamics, we expect similar transport behaviour may ex-

ist for other quasi-particles in solid. We focus on phonons here. Poiseuille flow and the propagation of second sound have been studied in graphene and similar 2D materials by numerically solving the semiclassical Boltzmann equation with inputs from density functional theory calculation^{10,11}. It is suggested that, contrary to three-dimensional materials^{2,31-36}, hydrodynamic phonon transport in 2D materials persists over a much larger temperature range (50 ~ 150 K) in micrometer scale samples. The quadratic dispersion of graphene ZA acoustic phonon mode is argued to play an important role in widening the temperature range¹¹.

However, unlike electrons, experimental evidence of phonon hydrodynamic transport in 2D materials has not been observed, despite recent progress in 3D materials^{34,35}. Theoretical analysis based on simplified models may help to identify possible experimental signatures of phonon hydrodynamics. Considering its universal behavior, it is interesting to ask whether similar effects observed for electrons can be expected for phonons. Here, we answer this question from the analysis of a Guyer-Krumhansl (G-K) equation for 2D materials, which we derive from the Peierls-Boltzmann equation with the Callaway model. Importantly, we consider both linear and quadratic acoustic phonon dispersion, which is critical to 2D materials. We extend the multiscale expansion technique⁹ to include both linear and quadratic phonon modes in 2D materials. This has not been considered before. We show that the G-K equation takes a familiar form, but the transport coefficients differ from normal Debye model, which assumes linear dispersion of acoustic phonon modes. The viscosity coefficients, the second sound velocity become temperature dependent, contrary to the Debye model. Our results will be useful for further theoretical and experimental study of phonon hydrodynamics in 2D materials.

The paper is organized as follows. The Sec. II we introduce our model and sketch the derivation of the 2D G-K equation. The technique details are presented in Appendix A. As limiting cases, in Sec. III, we show that our result predicts second sound propagating and Poiseuille flow, which have been studied previously by numerical calculations^{10,11}. In Sec. IV, as our new prediction, we

show that negative nonlocal heat conductance and heat current cortices may appear in ribbons of 2D materials with local heat current injection. Our conclusions are given in Sec. V.

II. THE 2D G-K EQUATION

We consider a prototype 2D material. It has one out-of-plane acoustic mode with a quadratic dispersion $\omega_k = ak^2$ (ZA mode), and two degenerate linear acoustic modes $\omega_k = v_g k$ (longitudinal and transverse). The magnitude of the linear group velocity is v_g , and the magnitude of the wave vector is $k = |\vec{k}|$. Here, in the spirit of Debye model, we ignore the possible anisotropic property and the difference between longitudinal and transverse branches. We will focus on the effect of ZA mode's quadratic dispersion on the hydrodynamic behavior.

We first sketch the derivation of the 2D G-K equation^{37,38}. Our starting point is the Peierls-Boltzmann equation under Callaway approximation^{39,40}

$$\frac{\partial f_{s\vec{k}}}{\partial t} + \vec{v}_{s\vec{k}} \cdot \nabla f_{s\vec{k}} = -\frac{f_{s\vec{k}} - f_{R,s\vec{k}}^{eq}}{\tau_R} - \frac{f_{s\vec{k}} - f_{N,s\vec{k}}^{eq}}{\tau_N}. \quad (1)$$

Here, s is the phonon index, τ_N is the constant relaxation time for the N-process, while τ_R is that for the resistive scattering process (R-process). It includes all scattering mechanisms that do not conserve crystal momentum, i. e., impurity scattering, phonon-scattering and other U-processes. We take the same τ_R and τ_N for all phonon branches, i.e., taking the wave vector and branch averaged values. This is the so-called gray approximation.

The N-process drives the system towards a displaced distribution function

$$f_{N,s\vec{k}}^{eq} = \left[e^{\beta_B (\hbar\omega_{s\vec{k}} - \hbar\vec{k} \cdot \vec{u})} - 1 \right]^{-1}, \quad (2)$$

with $\beta_B = (k_B T)^{-1}$, and \vec{u} is the drift velocity. But the R-process drives the system to an equilibrium Bose-Einstein distribution

$$f_{R,s\vec{k}}^{eq} = (e^{\beta_B \hbar\omega_{s\vec{k}}} - 1)^{-1}. \quad (3)$$

It has been shown numerically that, within some moderate temperature range (~ 100 K for graphene), the N-process is orders of magnitude faster than the R-process, meaning $\tau_R \gg \tau_N$ ^{10,11}. When the system size is much larger than the normal-scattering mean free path $l \approx v_g \tau_N$. The relaxation from local to global equilibrium or steady state is governed by hydrodynamic equations describing the conserved quantities during the N-process, including energy and crystal momentum.

As we know, conservation laws play central roles in the derivation of hydrodynamic equations. We consider energy and crystal momentum conservation here. Both

normal (N) and resistive (R) scattering processes conserve total energy, giving

$$\sum_s \int \frac{d\vec{k}}{(2\pi)^2} \hbar\omega_{s\vec{k}} f_{s\vec{k}} = \sum_s \int \frac{d\vec{k}}{(2\pi)^2} \hbar\omega_{s\vec{k}} f_{N,s\vec{k}}^{eq}, \quad (4)$$

$$\sum_s \int \frac{d\vec{k}}{(2\pi)^2} \hbar\omega_{s\vec{k}} f_{s\vec{k}} = \sum_s \int \frac{d\vec{k}}{(2\pi)^2} \hbar\omega_{s\vec{k}} f_{R,s\vec{k}}^{eq}, \quad (5)$$

while only the N-process obeys crystal momentum conservation, giving

$$\sum_s \int \frac{d\vec{k}}{(2\pi)^2} \hbar\vec{k} f_{s\vec{k}} = \sum_s \int \frac{d\vec{k}}{(2\pi)^2} \hbar\vec{k} f_{N,s\vec{k}}^{eq}. \quad (6)$$

To get the equation governing the dynamics of the conserved quantity, we multiply by $\hbar\omega_{s\vec{k}}$, integrate over \vec{k} and sum over the phonon index on both sides of Eq. (1). We then arrive at an equation describing energy conservation

$$\frac{\partial E}{\partial t} + \nabla \cdot \vec{q} = 0, \quad (7)$$

where

$$E = \sum_s \int \frac{d\vec{k}}{(2\pi)^2} \hbar\omega_{s\vec{k}} f_{s\vec{k}} \quad (8)$$

is the total energy density, and

$$\vec{q} = \sum_s \int \frac{d\vec{k}}{(2\pi)^2} \hbar\omega_{s\vec{k}} \vec{v}_{s\vec{k}} f_{s\vec{k}} \quad (9)$$

is the heat current density. The right hand side of Eq. (7) is zero because the scattering processes conserve energy.

In principle, we can write down similar equation for the crystal momentum density \vec{p} and its flux from its conservation law during N-processes. The G-K equation can be derived from the resulting momentum balance equation. This works well for the Debye model with linear phonon dispersion. But for graphene-like 2D system, the presence of quadratic dispersion leads to a divergent momentum flux, making further derivation difficult⁴¹. To avoid this, we consider the heat flux directly, i.e., multiplying $\hbar\omega\vec{v}$ to each term in Eq. (1) and summing over all wave vectors and phonon indices. This leads to

$$\frac{\partial \vec{q}}{\partial t} + \frac{\vec{\kappa}}{\tau_R} \cdot \nabla T = -\frac{\vec{q}}{\tau_R} - \frac{\vec{q}_1}{\tau_N}. \quad (10)$$

Here, \vec{q}_1 is the 1st order term of heat flux, which will be explained below. We have also defined a thermal conductivity tensor as

$$\vec{\kappa} = \tau_R \sum_s \int \frac{d\vec{k}}{(2\pi)^2} \hbar\omega_{s\vec{k}} \vec{v}_{s\vec{k}} \vec{v}_{s\vec{k}} \frac{\partial f_{s\vec{k}}}{\partial T}. \quad (11)$$

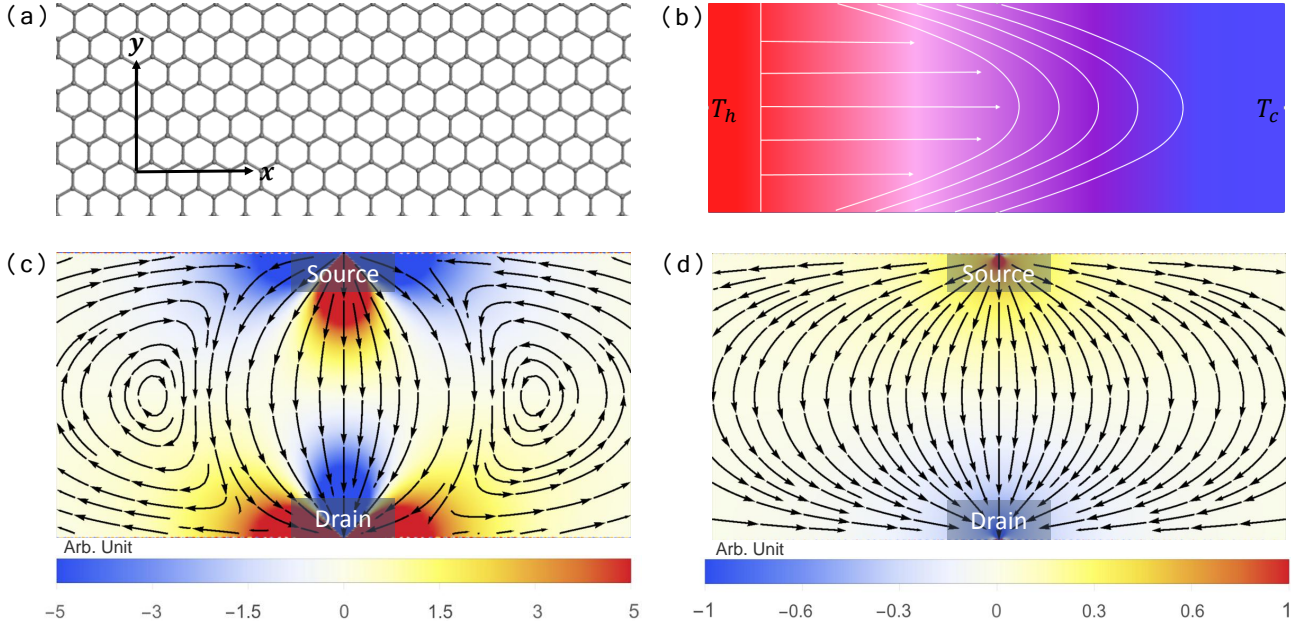


FIG. 1. (a) A graphene nano-ribbon as a prototype 2D materials showing hydrodynamics phonon transport. (b) Schematic of Poiseuille flow generated by the temperature difference along the nano-ribbon. The heat flux has a parabolic distribution across the ribbon. (c) Heat current loops (lines) and temperature distribution (color) due to the viscosity of the phonon gas as signature of hydrodynamic heat transport. We set $\epsilon = 1$. (d) The same as (c), but in the diffusive Fourier transport regime with $\epsilon = 300$.

To obtain the hydrodynamic equation, we rely on a multi-scale expansion technique developed recently⁹. The expansion is over both space and time as follows:

$$\frac{\partial}{\partial t} = \epsilon \frac{\partial}{\partial t_1} + \epsilon^2 \frac{\partial}{\partial t_2}, \quad (12)$$

$$\frac{\partial}{\partial x_i} = \epsilon \frac{\partial}{\partial x_{1i}}. \quad (13)$$

It is a perturbation expansion over a natural small parameter

$$\epsilon = \frac{\tau_N}{\tau_R}. \quad (14)$$

That is to say, we consider the situation where the scattering rates of N-process is much larger than that of R-process. We expand the phonon distribution as follows

$$f = f_0 + \epsilon f_1 + \epsilon^2 f_2 + \dots, \quad (15)$$

with f_0, f_1, f_2 the 0th, 1st and 2nd order terms of phonon distribution function. The macroscopic variables can be

expressed by the sum of approximate components

$$E = E_0 + \epsilon E_1 + \epsilon^2 E_2 + \dots,$$

$$E_n = \sum_s \int \hbar \omega_{s\vec{k}} f_{n,s\vec{k}} \frac{d\vec{k}}{(2\pi)^2}.$$

$$\vec{q} = \vec{q}_0 + \epsilon \vec{q}_1 + \epsilon^2 \vec{q}_2 + \dots,$$

$$\vec{q}_n = \sum_s \int \vec{v}_{s\vec{k}} \hbar \omega_{s\vec{k}} f_{n,s\vec{k}} \frac{d\vec{k}}{(2\pi)^2}.$$

$$\vec{\kappa} = \vec{\kappa}_0 + \epsilon \vec{\kappa}_1 + \epsilon^2 \vec{\kappa}_2 + \dots,$$

$$\vec{\kappa}_n = \tau_R \sum_s \int \hbar \omega_{s\vec{k}} \vec{v}_{s\vec{k}} \vec{v}_{s\vec{k}} \frac{\partial f_{n,s\vec{k}}}{\partial T} \frac{d\vec{k}}{(2\pi)^2}.$$

We include the 0th and 1st order terms with $\vec{q} \approx \vec{q}_0 + \epsilon \vec{q}_1$, $\vec{\kappa} \approx \vec{\kappa}_0 + \epsilon \vec{\kappa}_1$. According to energy conservation (Eq. (4)), we know that $E = E_0$, since $E_n = 0$ for $n > 0$. All these are calculated from the distribution function $f \approx f_0 + \epsilon f_1$, with $f_0 = f_N^{eq}$, $f_1 = f_R^{eq} - f_N^{eq} - \tau_N (\partial_{t_1} f_N^{eq} + v_i \partial_{x_{1i}} f_N^{eq})$. When \vec{u} is small, we can approximate f_N^{eq} as

$$f_N^{eq} \approx f_R^{eq} + \hbar \beta_B f_R^{eq} (f_R^{eq} + 1) \vec{k} \cdot \vec{u}. \quad (16)$$

Numerical calculation shows that this is indeed a good

approximation¹¹. Taking into account only the 0th order term f_0 , we can get

$$E = \frac{2(k_B T)^3}{\pi(\hbar v_g)^2} Zeta(3) + \frac{\pi(k_B T)^2}{24\hbar a} \equiv E_L + E_N, \quad (17)$$

$$\vec{q}_0 = \frac{3(k_B T)^3}{\pi(\hbar v_g)^2} Zeta(3)\vec{u} + \frac{\pi(k_B T)^2}{12\hbar a}\vec{u} \equiv \vec{q}_{0L} + \vec{q}_{0N}, \quad (18)$$

$$\vec{\kappa}_0 = \frac{6Zeta(3)k_B^3 T^2}{\pi\hbar^2}\tau_R\vec{I} = C_L v_g^2 \tau_R \vec{I}. \quad (19)$$

Here, E_L , E_N are the equilibrium energy density of the linear and quadratic phonon modes, respectively. \vec{q}_{0L} , \vec{q}_{0N} are the 0th order contribution of the linear and quadratic modes to the heat flux. They are both proportional to the drift velocity \vec{u} . $C_L = (\partial E_L / \partial T) = \frac{6Zeta(3)k_B^3}{\pi(\hbar v_g)^2} T^2$ is the specific heat capacity of the linear modes, C_N is defined similarly, and $C = C_L + C_N$.

The first-order result of macroscopic variables are

$$E_1 = 0, \quad (20)$$

$$\vec{q}_1 = 0, \quad (21)$$

$$\vec{\kappa}_1 = \tau_R \frac{\partial \vec{Q}}{\partial T} = \tau_R (\nabla \cdot \vec{Q}) \frac{1}{\nabla T}. \quad (22)$$

The expression of \vec{Q} and calculation details can be found in the Appendix. We arrive at the G-K equation of 2D materials

$$\frac{\partial \vec{q}}{\partial t} + \frac{\kappa_0}{\tau_R} \nabla T + \frac{1}{\tau_R} \vec{q} = \eta [\nabla^2 \vec{q} + 2\nabla(\nabla \cdot \vec{q})] - \zeta \nabla(\nabla \cdot \vec{q}). \quad (23)$$

We have defined the 0th order thermal conductivity as $\kappa_0 = \alpha C_L v_g^2 \tau_R$, the first and second viscosity coefficients as $\eta = \beta v_g^2 \tau_N$, $\zeta = \gamma v_g^2 \tau_N$, with $\alpha = 1$, $\beta = \frac{9E_L}{4(3E_L + 4E_N)}$, $\gamma = C_L / C$, respectively. Equation (23) with the above defined coefficients is the central results of this work. We can see that, although the form of the G-K equation is the same as the 3D case, the inclusion of quadratic phonon mode changes its coefficients. Notably, η and γ become temperature dependent, while for Debye model with three degenerate linear acoustic phonons modes, the coefficients are constant, with $\alpha = 1/3$, $\beta = 1/5$, $\gamma = 1/3$ for 3D and $\alpha = 1/2$, $\beta = 1/4$, $\gamma = 1/2$ for 2D case, respectively. In the following, we will analyze the consequences of this equation.

III. SECOND SOUND AND POISEUILLE FLOW

We now analyze the consequence of Eq. (23). In this section, we show that, the numerical results in previous studies^{10,11} can be obtained from Eq. (23) as special cases.

A. Second sound

The right side (RHS) of the G-K equation represents the effect of viscosity on the heat transport behavior. They come from the first order term in the expansion over ε . Before looking into these terms, we show here that the propagation of second sound can be analyzed without these terms. Replacing the RHS with zero, combining with Eq. (7), we arrive at

$$\frac{\partial^2 T}{\partial t^2} + \frac{1}{\tau_R} \frac{\partial T}{\partial t} - v_{ss}^2 \nabla^2 T = 0, \quad (24)$$

where we have defined the second sound velocity

$$v_{ss}^2 = \frac{\kappa_0}{C\tau_R} = \alpha\gamma v_g^2. \quad (25)$$

This is the wave equation describing propagation of second sound with velocity v_{ss} and damping coefficient τ_R^{-1} . For 3D materials with the Debye model, the second sound velocity $v_{ss} = v_g / \sqrt{3}$, similar model for 2D material gives $v_{ss} = v_g / \sqrt{2}$. Here, the presence of quadratic dispersion makes v_{ss} temperature dependent, inherited from the different temperature dependence of C_L and C_N .

B. Poiseuille flow

We now include the RHS of the G-K equation, and consider a nano-ribbon with length L ($0 \leq x \leq L$) and width w ($0 \leq y \leq w$) [Fig. 1 (a)]. A temperature difference is applied along the ribbon (x direction) [Fig. 1 (b)]. At steady state, ignoring \vec{q}/τ_R , Eq. (23) reduces to a one-dimension form $\frac{\partial^2 q}{\partial y^2} = A$. This gives rise to a parabolic heat flux distribution perpendicular to the flow $q(y) = \frac{A}{2}y(y-w)$, with $A = (\partial T / \partial x)\kappa_0 / \tau_R \eta$, if we assume a non-slip boundary condition $q(0) = q(w) = 0$. By integration over y , the heat current is obtained

$$I = \int_0^w q(y) dy = -\frac{1}{12} A w^3. \quad (26)$$

The negative sign means heat flows opposite to the temperature gradient. The heat current scaling as w^3 is a signature of the Poiseuille flow. For diffusive phonon transport, the heat current scales linearly with the ribbon width $I \propto w$, while for ballistic transport, the heat current can not go higher than linear scaling with the width. Thus, the cubic (super-linear) dependence of I on w can in principle be used as a signature of the Poiseuille flow. The Poiseuille flow in graphene ribbons has been studied numerically by solving the Boltzmann equation directly in Refs. 10 and 11. Similar behavior is also predicted for electronic transport in graphene nano-ribbons¹². Length and width dependent thermal conductivity in suspended single layer graphene has been reported experimentally^{42,43}. Thus, experimental confirmation of Poiseuille flow in graphene is already within reach.

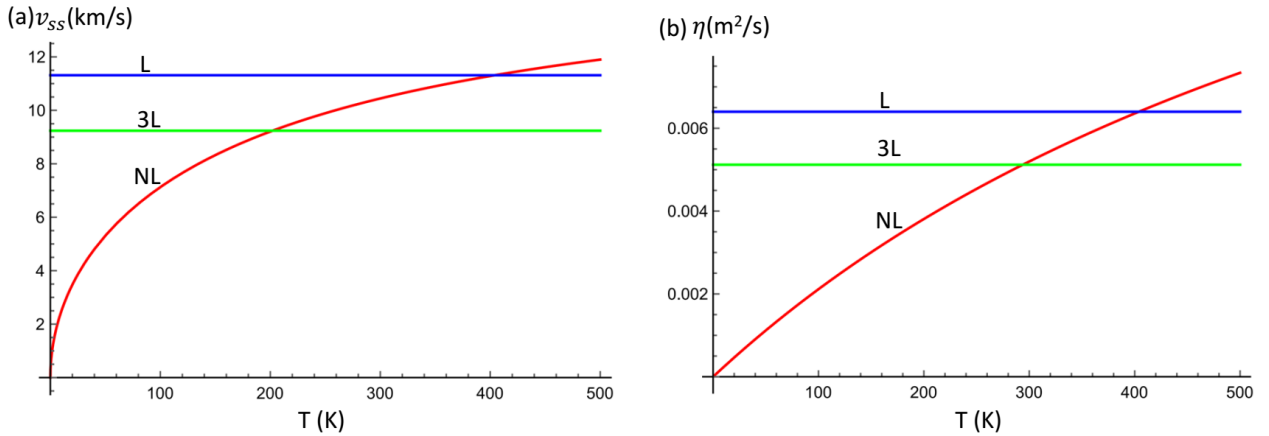


FIG. 2. (a) The second sound velocity v_{ss} as a function of temperature (T) for three different situations. (b) The dependence of the first viscosity coefficient η on temperature (T). Here, we take the $\tau_N = 10^{-10}$ s. NL stands for the 2D material with one quadratic ZA mode and two degenerate linear acoustic modes (longitudinal and transverse). L represents the 2D material with three degenerate linear acoustic phonons modes (2D Debye model). 3L means 3D material with three linear degenerate acoustic phonon modes (3D Debye model).

IV. HEAT CURRENT VORTICES AND NEGATIVE NONLOCAL CONDUCTANCE

One important consequence of Eq. (23) is nonlocal heat transport and formation of heat current vortices when there is a heat current source injecting into the 2D materials. As far as we know, this has not been considered before. To show this, we consider steady state transport in a setup sketched in Fig. 1 (c). Heat current source and drain are attached to a graphene nano-ribbon. The pattern of current flow at steady state can be obtained from the solution of simplified version of Eq. (23). At steady state, according to Eq. (7), we have $\partial \vec{q} / \partial t = \partial E / \partial t = 0$. The resulting equation has the form

$$\eta \nabla^2 \vec{q} - \tau_R^{-1} \vec{q} = C_L v_g^2 \nabla T. \quad (27)$$

It shares the same form as the electronic case in Ref. 12. The 1st term on the left hand side (LHS) is the hydrodynamic term due to viscosity. It is the origin of the nonlocal transport behavior. When τ_R^{-1} is negligible, we get pure hydrodynamic viscous flow. On the other hand, when η is negligible, we recover the normal diffusive heat transport governed by Fourier law. Thus, equation 27 applies to steady state diffusive and hydrodynamic transport. Actually, it is suggestive to define a dimensionless parameter

$$\epsilon = \frac{w^2}{\eta \tau_R} = \frac{w^2}{\beta v_g^2 \tau_N \tau_R} \quad (28)$$

to characterize the relative contribution of diffusive and hydrodynamic transport.

As an example, we have plotted typical heat current flow patterns (lines) and the resulting temperature distribution (color) with $\epsilon = 1$ and 300 in Fig. 1 (c) and (d),

respectively. Here, a flow of heat current from a point source $I(x) = I\delta(x)$ is injected into the ribbon and collected at the opposite side. The non-slip boundary condition is used to solve Eq. (27). The heat current flow within the ribbon can be obtained by solving Eq. (27) with the help of the streaming function. In Fig. 1 (c), hydrodynamic transport is dominant. The formation of vortices besides both sides of the direct source-to-drain flow is a characteristic feature of the viscous flow. Another prominent feature is the ‘separation’ of temperature gradient and heat flow. Even negative thermal resistance can be observed, where the heat current flows from the low to the high temperature regime. In Fig. 1 (d), the diffusive Fourier transport becomes dominant. Heat current vortices and negative resistance are absent. Thus, we can study the transition from hydrodynamic to Fourier transport by changing the magnitude of ϵ .

We now give an order-of-magnitude analysis using parameters of graphene. We obtain the phonon dispersion relation of graphene using density function theory based calculations⁴⁴. Fitting the dispersion relation results in $v_g = 1.6 \times 10^4$ m/s for the linear modes, $a = 5.5 \times 10^{-7}$ m²/s for the quadratic mode. The specific heat capacity of them is given by $C_L = \frac{6\text{Zeta}(3)}{\pi} \frac{k_B^3 T^2}{(\hbar v_g)^2} \approx 2.14 \times 10^{-9} T^2$ Jm⁻²K⁻¹ and $C_N = \frac{\pi}{12} \frac{k_B^2 T}{\hbar a} \approx 8.63 \times 10^{-7} T$ Jm⁻²K⁻¹, respectively. To estimate the transport coefficients and the dimensionless factor ϵ , we use $\tau_N = 10^{-10}$ s, $\tau_R = 10^{-7}$ s¹¹. We get $\beta \approx 0.08$ at $T = 100$ K, smaller than value obtained from the 2D Debye model $\beta = 1/4$. The different temperature dependence of C_L , C_N and E_L , E_N gives rise to temperature dependent v_{ss} and η . This is contrast to 2D or 3D Debye model. The comparison of different situations is shown in Fig. 2 (a) and (b) for v_{ss} and η , respectively. We find that, the presence of

quadratic ZA mode reduces v_{ss} and η in the relevant temperature ~ 100 K. Still, we get $\eta \approx 0.002 \text{ m}^2/\text{s}$ at $T = 100$ K, which is orders of magnitude larger than that of water. We also get the dimensionless parameter $\epsilon \approx 5 \times 10^9 \omega^2 \text{ m}^{-2}$. Thus, phonon hydrodynamic transport can be realized in high quality graphene nanoribbons of micrometer scale. The plot in Fig. 1 (c) with $\epsilon = 1$ corresponds to sample length of $\sim 15 \text{ }\mu\text{m}$.

V. CONCLUSIONS

In summary, we have derived a 2D version of the G-K equation describing hydrodynamic phonon heat transport. We take into account the out of plane quadratic phonon dispersion of the ZA mode, normally present in 2D materials. Its effect on the hydrodynamic transport is analyzed. The derived equation serves as a starting point for investigating nonlocal hydrodynamic phonon transport behavior in 2D materials. It shares similar form as the Navier-Stokes equation that has been used to study

electron hydrodynamic transport in graphene. Many interesting transport behaviors, including nonlocal negative resistance, higher-than-ballistic transport, predicted for electrons can be studied by phonons. Moreover, a large overlap of the parameter regime between electron and phonon hydrodynamic transport in graphene makes it promising to study the effect of their mutual interaction on the thermal transport behavior of the two kinds of fluids.

During the submission of present work, several new studies came out⁴⁵⁻⁴⁷, which are all based on numerical calculations and complementary to present analytical study.

ACKNOWLEDGMENTS

The authors thank Nuo Yang, Jin-Hua Gao for discussions. We acknowledge financial support from National Natural Science Foundation of China (Grant No. 21873033).

Appendix A: Derivation of the 2D G-K equation

Here, we give the derivation of Eq. (23) in the main text. We use the recent developed multiscale expansion technique⁹. The expansion is over both space and time as follows:

$$\frac{\partial}{\partial t} = \epsilon \frac{\partial}{\partial t_1} + \epsilon^2 \frac{\partial}{\partial t_2}, \quad (\text{A1})$$

$$\frac{\partial}{\partial x_i} = \epsilon \frac{\partial}{\partial x_{1i}}, \quad (\text{A2})$$

where ϵ is a small parameter, defined as

$$\epsilon = \frac{\tau_N}{\tau_R}. \quad (\text{A3})$$

That is to say, we consider the situation where the scattering rates of N-process is much larger than that of R-process, preferential for hydrodynamic phonon transport. We expand the phonon distribution function as follows

$$f = f_0 + \epsilon f_1 + \epsilon^2 f_2 + \dots, \quad (\text{A4})$$

with f_0, f_1, f_2 the 0th, 1st and 2nd order terms of phonon distribution function. The macroscopic variables can be expressed by the sum of approximate components

$$E = E_0 + \epsilon E_1 + \epsilon^2 E_2 + \dots, \quad E_n = \sum_s \int \hbar \omega_{s\vec{k}} f_{n,s\vec{k}} \frac{d\vec{k}}{(2\pi)^2}, \quad (\text{A5})$$

$$\vec{q} = \vec{q}_0 + \epsilon \vec{q}_1 + \epsilon^2 \vec{q}_2 + \dots, \quad \vec{q}_n = \sum_s \int \vec{v}_{s\vec{k}} \hbar \omega_{s\vec{k}} f_{n,s\vec{k}} \frac{d\vec{k}}{(2\pi)^2}, \quad (\text{A6})$$

$$\vec{\kappa} = \vec{\kappa}_0 + \epsilon \vec{\kappa}_1 + \epsilon^2 \vec{\kappa}_2 + \dots, \quad \vec{\kappa}_n = \tau_R \sum_s \int \hbar \omega_{s\vec{k}} \vec{v}_{s\vec{k}} \vec{v}_{s\vec{k}} \frac{\partial f_{n,s\vec{k}}}{\partial T} \frac{d\vec{k}}{(2\pi)^2}. \quad (\text{A7})$$

Substituting all of the equations above into the Peierls-Boltzmann equation, we obtain the 0th and 1st order terms of phonon distribution function:

$$f_0 = f_N^{eq}, \quad (\text{A8})$$

$$f_1 = f_R^{eq} - f_N^{eq} - \tau_N \left(\frac{\partial f_N^{eq}}{\partial t_1} + v_i \frac{\partial f_N^{eq}}{\partial x_{1i}} \right), \quad (\text{A9})$$

and different order of approximations for the balance equations

$$\frac{\partial E}{\partial t_1} + \frac{\partial}{\partial x_{1i}} q_{0i} = 0, \quad (\text{A10})$$

$$\frac{\partial E}{\partial t_2} + \frac{\partial}{\partial x_{1i}} q_{1i} = 0, \quad (\text{A11})$$

$$\frac{\partial q_{0i}}{\partial t_1} + \kappa_{0ij} \frac{\partial T}{\partial x_{1j}} = -\frac{1}{\tau_N} q_{0i} - \frac{1}{\tau_N} q_{1i}, \quad (\text{A12})$$

$$\frac{\partial q_{0i}}{\partial t_2} + \frac{\partial q_{1i}}{\partial t_1} + \kappa_{1ij} \frac{\partial T}{\partial x_{1j}} = -\frac{1}{\tau_N} q_{1i} - \frac{1}{\tau_N} q_{2i}. \quad (\text{A13})$$

1. The zeroth-order result

We calculate the macroscopic variables including the energy density, the heat flux and the thermal conductivity, taking into account the 0th order term f_0 . We make the following approximation

$$f_0 = f_N^{eq} = f_R^{eq} + f_{N1}^{eq} \approx f_R^{eq} + \beta_B f_R^{eq} (f_R^{eq} + 1) \hbar \vec{k} \cdot \vec{u}, \quad (\text{A14})$$

whose validity has been checked numerically¹¹.

a. Energy density

We consider the phonon energy density first. According to energy conservation (4), we know that $E = E_0$,

$$E = \sum_s \int \hbar \omega_{s\vec{k}} f_{N,s\vec{k}}^{eq} \frac{d\vec{k}}{(2\pi)^2} = \sum_s \int \hbar \omega_{s\vec{k}} f_{R,s\vec{k}}^{eq} \frac{d\vec{k}}{(2\pi)^2} + \sum_s \int \hbar \omega_{s\vec{k}} f_{R,s\vec{k}}^{eq} \left(1 + f_{R,s\vec{k}}^{eq}\right) \frac{\hbar \vec{k} \cdot \vec{u}}{k_B T} \frac{d\vec{k}}{(2\pi)^2}. \quad (\text{A15})$$

The second term in the above equation vanishes because it's an odd function of \vec{k} . Thus we arrive at:

$$E = \sum_s \int \hbar \omega_{s\vec{k}} f_{R,s\vec{k}}^{eq} \frac{d\vec{k}}{(2\pi)^2} = \frac{2}{\pi} \frac{(k_B T)^3}{(\hbar v_g)^2} \text{Zeta}(3) + \frac{\pi}{24} \frac{(k_B T)^2}{\hbar a} \equiv E_L + E_N. \quad (\text{A16})$$

Here, E_L and E_N are the energy density of linear and quadratic phonon modes, respectively. Note that we have included the factor 2 to account the degeneracy of the linear phonon modes.

b. Heat flux

The 0th order heat flux is calculated as

$$\vec{q}_0 = \sum_s \int \vec{v}_{s\vec{k}} \hbar \omega_{s\vec{k}} f_{N,s\vec{k}}^{eq} \frac{d\vec{k}}{(2\pi)^2} = \sum_s \int \vec{v}_{s\vec{k}} \hbar \omega_{s\vec{k}} f_{R,s\vec{k}}^{eq} \frac{d\vec{k}}{(2\pi)^2} + \sum_s \int \vec{v}_{s\vec{k}} \hbar \omega_{s\vec{k}} f_{N1,s\vec{k}}^{eq} \frac{d\vec{k}}{(2\pi)^2}. \quad (\text{A17})$$

Since at thermal equilibrium, the heat flux is zero. Only the second term contributes

$$\vec{q}_0 = \sum_s \int \vec{v}_{s\vec{k}} \hbar \omega_{s\vec{k}} f_{N1,s\vec{k}}^{eq} \frac{d\vec{k}}{(2\pi)^2} = \frac{3}{\pi} \frac{(k_B T)^3}{(\hbar v_g)^2} \text{Zeta}(3) \vec{u} + \frac{\pi}{12} \frac{(k_B T)^2}{\hbar a} \vec{u} \equiv \vec{q}_{0L} + \vec{q}_{0N}. \quad (\text{A18})$$

Here, \vec{q}_{0L} , \vec{q}_{0N} are the 0th order contribution of the linear and quadratic modes to the heat flux.

c. Thermal conductivity tensor

The thermal conductivity tensor is

$$\vec{\kappa}_0 = \tau_R \sum_s \int \hbar \omega_{s\vec{k}} \vec{v}_{s\vec{k}} \vec{v}_{s\vec{k}} \frac{\partial f_{N,s\vec{k}}^{eq}}{\partial T} \frac{d\vec{k}}{(2\pi)^2} = \tau_R \sum_s \int \hbar \omega_{s\vec{k}} \vec{v}_{s\vec{k}} \vec{v}_{s\vec{k}} \frac{\partial f_{R,s\vec{k}}^{eq}}{\partial T} \frac{d\vec{k}}{(2\pi)^2} + \tau_R \sum_s \int \hbar \omega_{s\vec{k}} \vec{v}_{s\vec{k}} \vec{v}_{s\vec{k}} \frac{\partial f_{N1,s\vec{k}}^{eq}}{\partial T} \frac{d\vec{k}}{(2\pi)^2}. \quad (\text{A19})$$

Likewise, the second term in the above equation is an odd function of \vec{k} and thus is zero. We then have

$$\begin{aligned}\vec{\kappa}_0 &= \tau_R \sum_s \int \hbar \omega_{s\vec{k}} \vec{v}_{s\vec{k}} \vec{v}_{s\vec{k}} \frac{\partial f_{R,s\vec{k}}^{eq}}{\partial T} \frac{d\vec{k}}{(2\pi)^2} = \tau_R \sum_s \int \hbar \omega_{s\vec{k}} \vec{v}_{s\vec{k}} \vec{v}_{s\vec{k}} f_{R,s\vec{k}}^{eq} \left(f_{R,s\vec{k}}^{eq} + 1 \right) \frac{\hbar \omega_{s\vec{k}}}{k_B T^2} \frac{d\vec{k}}{(2\pi)^2} \\ &= \frac{3}{\pi} \frac{k_B^3 T^2}{\hbar^2} \text{Zeta}(3) \tau_R \vec{I} + \frac{3}{\pi} \frac{k_B^3 T^2}{\hbar^2} \text{Zeta}(3) \tau_R \vec{I} \equiv \vec{\kappa}_{0L} + \vec{\kappa}_{0N}.\end{aligned}\quad (\text{A20})$$

We get the 0th order thermal conductivity contributed from the linear $\vec{\kappa}_{0L}$ and quadratic modes $\vec{\kappa}_{0N}$. It is noted that, given a constant τ_R , the thermal conductivity contributed from a quadratic mode is two times larger than that contributed from a linear mode. Both of them are independent of the details of the dispersion. So we can rewrite κ_0 in terms of the energy density of the linear phonon modes,

$$\vec{\kappa}_0 = \frac{6 \text{Zeta}(3)}{\pi} \frac{k_B^3 T^2}{\hbar^2} \tau_R \vec{I} = C_L v_g^2 \tau_R \vec{I}, \quad (\text{A21})$$

where the specific heat capacity of the linear modes is:

$$C_L = \frac{\partial E_L}{\partial T} = \frac{6 \text{Zeta}(3)}{\pi} \frac{k_B^3}{(\hbar v_g)^2} T^2.$$

2. The first-order result

Now, we calculate the 1st order terms in the expansion

$$f_1 = f_R^{eq} - f_N^{eq} - \tau_N \left(\frac{\partial f_N^{eq}}{\partial t_1} + v_i \frac{\partial f_N^{eq}}{\partial x_{1i}} \right). \quad (\text{A22})$$

Based on the chain rule

$$\frac{\partial f_N^{eq}}{\partial t_1} = \frac{\partial f_N^{eq}}{\partial u_j} \frac{\partial u_j}{\partial t_1} + \frac{\partial f_N^{eq}}{\partial T} \frac{\partial T}{\partial t_1}, \quad (\text{A23})$$

$$\frac{\partial f_N^{eq}}{\partial x_{1i}} = \frac{\partial f_N^{eq}}{\partial u_j} \frac{\partial u_j}{\partial x_{1i}} + \frac{\partial f_N^{eq}}{\partial T} \frac{\partial T}{\partial x_{1i}}, \quad (\text{A24})$$

and the approximation for f_N^{eq} , combined with Eqs. (A10),(A11), we arrive at a lengthy expression for f_1 :

$$\begin{aligned}f_1 &= -\frac{\hbar \vec{k} \vec{u}}{k_B T} f_R^{eq} (f_R^{eq} + 1) - \tau_N f_R^{eq} (f_R^{eq} + 1) \left\{ \frac{\hbar k_i}{k_B T} \left(-\frac{2C_L v_g^2}{3E_L + 4E_N} \frac{\partial T}{\partial x_{1i}} + \frac{u_i}{3E_L + 4E_N} \frac{3C_L + 4C_N}{C} \frac{\partial q_{0j}}{\partial x_{1j}} - \right. \right. \\ &\left. \left. \frac{2}{3E_L + 4E_N} \frac{q_{0i}}{\tau_N} \right) + \left(\frac{v}{k} k_i \frac{\partial T}{\partial x_{1i}} - \frac{1}{C} \frac{\partial q_{0j}}{\partial x_{1j}} \right) \left[\frac{\hbar \omega}{k_B T^2} + \frac{\hbar \omega}{k_B T^2} (2f_R^{eq} + 1) \frac{\hbar \vec{k} \vec{u}}{k_B T} - \frac{\hbar \vec{k} \vec{u}}{k_B T^2} \right] + \frac{v}{k} \frac{\hbar k_i k_j}{k_B T} \frac{\partial}{\partial x_{1i}} \left(\frac{2q_{0j}}{3E_L + 4E_N} \right) \right\}. \quad (\text{A25})\end{aligned}$$

We notice from eqs. (A10-A13) that, f_1 depends on \vec{q}_1 , while to obtain \vec{q}_1 we need f_1 . In principle, we need to self-consistent calculations of them. Here, to arrive at analytical result, we made the truncation and set $\vec{q}_1 = 0$ in eqs. (A10-A13).

a. Phonon energy density

According to the foregoing discussion, we can get :

$$E = E_0. \quad (\text{A26})$$

The higher order terms of distribution function do not contribute to the energy density.

b. Heat flux

Using the truncation we made for f_1 , we can check that $\vec{q}_1 = 0$ if we plug Eq. (A25) into Eq. (A6)

$$\vec{q}_1 = \sum_s \int \hbar \omega_{s\vec{k}} \vec{v}_{s\vec{k}} f_{1,s\vec{k}} \frac{d\vec{k}}{(2\pi)^2} = \vec{q}_{1L} + \vec{q}_{1N} = 0, \quad (\text{A27})$$

as required by our truncation scheme.

c. Thermal conductivity tensor

Finally, we consider the thermal conductivity tensor. We consider the linear and quadratic modes separately

$$\vec{\kappa}_1 = \tau_R \frac{\partial}{\partial T} (\vec{Q}_L + \vec{Q}_N), \quad (\text{A28})$$

with \vec{Q}_L, \vec{Q}_N corresponding to the contribution from linear and quadratic modes, respectively. Again, the odd parts do not contribute to the integral. Collecting the even parts, we divide \vec{Q}_L into three parts:

$$\vec{Q}_L = \vec{Q}_{L,I} + \vec{Q}_{L,II} + \vec{Q}_{L,III}, \quad (\text{A29})$$

with each part written as

$$(Q_{L,I})_{mn} = \frac{1}{2} \tau_N v_g^2 \frac{C_L}{C} \frac{\partial q_{0j}}{\partial x_{1j}} \delta_{mn}, \quad (\text{A30})$$

$$(Q_{L,II})_{mn} = -\frac{3}{4} v_g^2 E_L \tau_N \left[\frac{\partial}{\partial x_{1i}} \left(\frac{q_{0i}}{3E_L + 4E_N} \right) \delta_{mn} + \frac{\partial}{\partial x_{1m}} \left(\frac{q_{0n}}{3E_L + 4E_N} \right) + \frac{\partial}{\partial x_{1n}} \left(\frac{q_{0m}}{3E_L + 4E_N} \right) \right], \quad (\text{A31})$$

$$(Q_{L,III})_{mn} = -\frac{3}{4} \frac{v_g^2 \tau_N}{T} \left[(q_{0L})_i \frac{\partial T}{\partial x_{1i}} \delta_{mn} + (q_{0L})_n \frac{\partial T}{\partial x_{1m}} + (q_{0L})_m \frac{\partial T}{\partial x_{1n}} \right]. \quad (\text{A32})$$

Similarly,

$$\vec{Q}_N = \vec{Q}_{N,I} + \vec{Q}_{N,II} + \vec{Q}_{N,III}, \quad (\text{A33})$$

with

$$(Q_{N,I})_{mn} = \frac{1}{2} \tau_N v_g^2 \frac{C_L}{C} \frac{\partial q_{0j}}{\partial x_{1j}} \delta_{mn}, \quad (\text{A34})$$

$$(Q_{N,II})_{mn} = -\frac{3}{4} v_g^2 E_L \tau_N \left[\frac{\partial}{\partial x_{1i}} \left(\frac{q_{0i}}{3E_L + 4E_N} \right) \delta_{mn} + \frac{\partial}{\partial x_{1m}} \left(\frac{q_{0n}}{3E_L + 4E_N} \right) + \frac{\partial}{\partial x_{1n}} \left(\frac{q_{0m}}{3E_L + 4E_N} \right) \right], \quad (\text{A35})$$

$$(Q_{N,III})_{mn} = -\frac{3}{2} \frac{v_g^2 \tau_N}{T} \left[(q_{0L})_i \frac{\partial T}{\partial x_{1i}} \delta_{mn} + (q_{0L})_n \frac{\partial T}{\partial x_{1m}} + (q_{0L})_m \frac{\partial T}{\partial x_{1n}} \right]. \quad (\text{A36})$$

Summing up the linear and nonlinear results gives

$$(Q_I)_{mn} = \tau_N v_g^2 \frac{C_L}{C} \frac{\partial q_{0j}}{\partial x_{1j}} \delta_{mn}, \quad (\text{A37})$$

$$(Q_{II})_{mn} = -\frac{9}{4} v_g^2 E_L \tau_N \left[\frac{\partial}{\partial x_{1i}} \left(\frac{q_{0i}}{3E_L + 4E_N} \right) \delta_{mn} + \frac{\partial}{\partial x_{1m}} \left(\frac{q_{0n}}{3E_L + 4E_N} \right) + \frac{\partial}{\partial x_{1n}} \left(\frac{q_{0m}}{3E_L + 4E_N} \right) \right], \quad (\text{A38})$$

$$(Q_{III})_{mn} = -\frac{9}{4} \frac{v_g^2 \tau_N}{T} \left[(q_{0L})_i \frac{\partial T}{\partial x_{1i}} \delta_{mn} + (q_{0L})_n \frac{\partial T}{\partial x_{1m}} + (q_{0L})_m \frac{\partial T}{\partial x_{1n}} \right], \quad (\text{A39})$$

and κ_1 is obtained from

$$\vec{\kappa}_1 = \tau_R \frac{\partial \vec{Q}}{\partial T} = \tau_R (\nabla \cdot \vec{Q}) \frac{1}{\nabla T}. \quad (\text{A40})$$

3. The G-K equation

Substituting the calculated 0th and 1st order results into Eq. (10), neglecting the nonlinear effects resulting from the product of heat flux and temperature gradient in κ_1 , we get the G-K equation

$$\frac{\partial \vec{q}}{\partial t} + \frac{\kappa_0}{\tau_R} \nabla T + \frac{1}{\tau_R} \vec{q} = \eta [\nabla^2 \vec{q} + 2\nabla(\nabla \cdot \vec{q})] - \zeta \nabla(\nabla \cdot \vec{q}). \quad (\text{A41})$$

The transport coefficients are $\kappa_0 = \alpha C_L v_g^2 \tau_R$, $\eta = \beta v_g^2 \tau_N$, $\xi = \gamma v_g^2 \tau_N$, with $\alpha = 1$, $\beta = \frac{9}{4} \frac{E_L}{3E_L + 4E_N}$, $\gamma = \frac{C_L}{C}$, respectively. For comparison, we also consider the 2D Debye model with three degenerate acoustic phonon modes. The resulting equation is the same, but with the coefficients $\alpha = \frac{1}{2}$, $\beta = \frac{1}{4}$, $\gamma = \frac{1}{2}$. These results can be compared with the 3D Debye model, resulting in $\alpha = \frac{1}{3}$, $\beta = \frac{1}{5}$, $\gamma = \frac{1}{3}$.

-
- ¹ R. N. Gurzhi, *Sov. Phys. Usp.* **11**, 255 (1968).
² H. Beck, P. F. Meier, and A. Thellung, *Phys. Stat. Sol. (a)* **24**, 11 (1974).
³ M. J. M. de Jong and L. W. Molenkamp, *Phys. Rev. B* **51**, 13389 (1995).
⁴ D. A. Bandurin, I. Torre, R. K. Kumar, M. B. Shalom, A. Tomadin, A. Principi, G. H. Auton, E. Khestanova, K. S. Novoselov, I. V. Grigorieva, L. A. Ponomarenko, A. K. Geim, and M. Polini, *Science* **351**, 1055 (2016).
⁵ J. Crossno, J. K. Shi, K. Wang, X. Liu, A. Harzheim, A. Lucas, S. Sachdev, P. Kim, T. Taniguchi, K. Watanabe, T. A. Ohki, and K. C. Fong, *Science* **351**, 1058 (2016).
⁶ P. J. W. Moll, P. Kushwaha, N. Nandi, B. Schmidt, and A. P. Mackenzie, *Science* **351**, 1061 (2016).
⁷ C. de Tomas, A. Cantarero, A. F. Lopeandia, and F. X. Alvarez, *J. Appl. Phys.* **115**, 164314 (2014).
⁸ A. Sellitto, I. Carlomagno, and D. Jou, *Proc. R. Soc. A* **471**, 20150376 (2015).
⁹ Y. Guo and M. Wang, *Phys. Rep.* **595**, 1 (2015).
¹⁰ A. Cepellotti, G. Fugallo, L. Paulatto, M. Lazzeri, F. Mauri, and N. Marzari, *Nat. Commun.* **6**, 6400 (2015).
¹¹ S. Lee, D. Broido, K. Esfarjani, and G. Chen, *Nat. Commun.* **6**, 6290 (2015).
¹² L. Levitov and G. Falkovich, *Nat. Phys.* **12**, 672 (2016).
¹³ C. Cao, E. Elliott, J. Joseph, H. Wu, J. Petricka, T. Schfer, and J. E. Thomas, *Science* **331**, 58 (2011).
¹⁴ B. V. Jacak and B. Müller, *Science* **337**, 310 (2012).
¹⁵ X. Gu, Y. Wei, X. Yin, B. Li, and R. Yang, *Rev. Mod. Phys.* **90**, 041002 (2018).
¹⁶ N. Li, J. Ren, L. Wang, G. Zhang, P. Hänggi, and B. Li, *Rev. Mod. Phys.* **84**, 1045 (2012).
¹⁷ J.-S. Wang, J. Wang, and J.-T. Lü, *Eur. Phys. J. B* **62**, 381 (2008).
¹⁸ J. Gooth, F. Menges, C. Shekhar, V. S. N. Kumar, Y. Sun, U. Drechsler, R. Zierold, C. Felser, and B. Gotsmann, *arXiv:1706.05925* (2017).
¹⁹ H. Guo, E. Ilseven, G. Falkovich, and L. Levitov, *PNAS* **114**, 3068 (2017).
²⁰ G. Falkovich and L. Levitov, *Phys. Rev. Lett.* **119**, 066601 (2017).
²¹ P. Alekseev, *Phys. Rev. Lett.* **117**, 166601 (2016).
²² F. M. D. Pellegrino, I. Torre, A. K. Geim, and M. Polini, *Phys. Rev. B* **94**, 155414 (2016).
²³ U. Briskot, M. Schtt, I. V. Gornyi, M. Titov, B. N. Narozhny, and A. D. Mirlin, *Phys. Rev. B* **92**, 115426 (2015).
²⁴ B. N. Narozhny, I. V. Gornyi, M. Titov, M. Schtt, and A. D. Mirlin, *Phys. Rev. B* **91**, 035414 (2015).
²⁵ A. Lucas and K. C. Fong, *J. Phys.: Condens. Matter* **30**, 053001 (2018).
²⁶ A. Cepellotti and N. Marzari, *Phys. Rev. X* **6**, 041013 (2016).
²⁷ A. Cepellotti and N. Marzari, *Phys. Rev. Materials* **1**, 045406 (2017).
²⁸ S. Lee and L. Lindsay, *Phys. Rev. B* **95**, 184304 (2017).
²⁹ Z. Ding, J. Zhou, B. Song, V. Chiloian, M. Li, T.-H. Liu, and G. Chen, *Nano Lett.* **18**, 638 (2018).
³⁰ Y. Guo and M. Wang, *Phys. Rev. B* **96**, 134312 (2017).
³¹ C. C. Ackerman, B. Bertman, H. A. Fairbank, and R. A. Guyer, *Phys. Rev. Lett.* **16**, 789 (1966).
³² V. Narayanamurti and R. C. Dynes, *Phys. Rev. Lett.* **28**, 1461 (1972).
³³ H. E. Jackson, C. T. Walker, and T. F. McNelly, *Phys. Rev. Lett.* **25**, 26 (1970).
³⁴ V. Martelli, J. L. Jiménez, M. Continentino, E. Baggio-Saitovitch, and K. Behnia, *Phys. Rev. Lett.* **120**, 125901 (2018).
³⁵ Y. Machida, A. Subedi, K. Akiba, A. Miyake, M. Tokunaga, Y. Akahama, K. Izawa, and K. Behnia, *Sci Adv* **4**, eaat3374 (2018).
³⁶ M. Markov, J. Sjakste, G. Barbarino, G. Fugallo, L. Paulatto, M. Lazzeri, F. Mauri, and N. Vast, *Phys. Rev. Lett.* **120**, 075901 (2018).
³⁷ R. A. Guyer and J. A. Krumhansl, *Phys. Rev.* **148**, 766 (1966).
³⁸ R. A. Guyer and J. A. Krumhansl, *Phys. Rev.* **148**, 778 (1966).
³⁹ J. Callaway, *Phys. Rev.* **113**, 1046 (1959).
⁴⁰ P. B. Allen, *Phys. Rev. B* **88**, 144302 (2013).
⁴¹ A. Cepellotti, *Thermal transport in low dimensions*, Ph.D. thesis, EPFL (2016).
⁴² M.-H. Bae, Z. Li, Z. Aksamija, P. N. Martin, F. Xiong, Z.-Y. Ong, I. Knezevic, and E. Pop, *Nat. Commun.* **4**, 1734 (2013).
⁴³ X. Xu, L. F. C. Pereira, Y. Wang, J. Wu, K. Zhang, X. Zhao, S. Bae, C. Tinh Bui, R. Xie, J. T. L. Thong, B. H. Hong, K. P. Loh, D. Donadio, B. Li, and B. Özyilmaz, *Nat. Commun.* **5**, 3689 (2014).
⁴⁴ For the density functional theory calculation, we use the Vienna Ab-initio Simulation Package and the generalized gradient approximation for the exchange-correlation functional. The parameters are the same as Ref. 48.

- ⁴⁵ C. Zhang, Z. Guo, and S. Chen, [International Journal of Heat and Mass Transfer](#) **130**, 1366 (2019).
- ⁴⁶ Y. Guo and M. Wang, [Phys. Rev. B](#) **97**, 035421 (2018).
- ⁴⁷ X. Li and S. Lee, [Phys. Rev. B](#) **97**, 094309 (2018).
- ⁴⁸ X.-J. Ge, K.-L. Yao, and J.-T. Lü, [Phys. Rev. B](#) **94**, 165433 (2016).